

"This is the peer reviewed version of the following article: „Photo-Organocatalytic Enantioselective Radical Cascade Enabled by Single-Electron Transfer Activation of Allenes“ which has been published in final form at DOI: 10.1002/adsc.201900973. This article may be used for non-commercial purposes in accordance with Wiley Terms and Conditions for Self-Archiving."

COMMUNICATION

Photo-Organocatalytic Enantioselective Radical Cascade Enabled by Single-Electron Transfer Activation of Allenes

Luca Alessandro Perego,^a Pablo Bonilla,^a and Paolo Melchiorre^{a,b*}

^a ICIQ – Institute of Chemical Research of Catalonia, the Barcelona Institute of Science and Technology, Avinguda Països Catalans 16, 43007 Tarragona, Spain

^b ICREA – Passeig Lluís Companys 23, 08010 Barcelona, Spain

*e-mail: pmelchiorre@icq.es

Dedicated to Professor Eric Jacobsen on the occasion of his 60th birthday

Received:



Supporting information for this article is available on the WWW under <http://dx.doi.org/10.1002/adsc.201900973>.

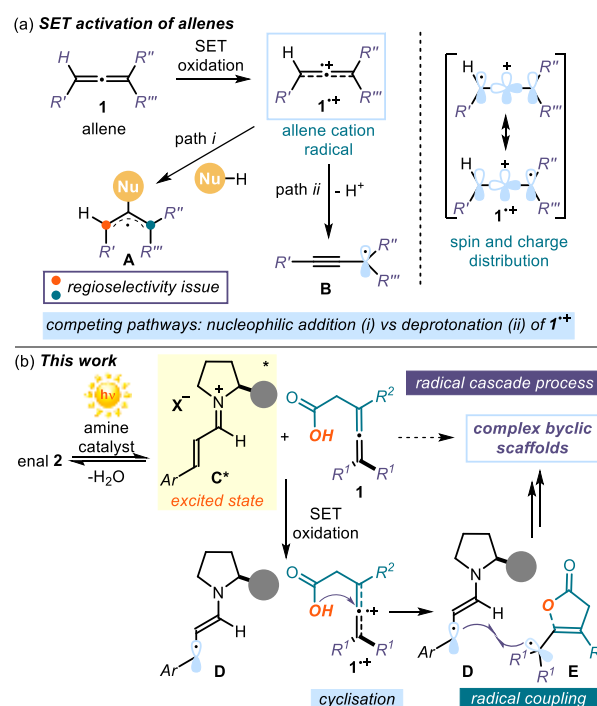
Abstract. Allenes are commonly used in metal-mediated transformations, cycloaddition reactions, and radical processes. However, their activation by single-electron transfer (SET) is largely underexplored. Herein, we report a **visible light-driven** enantioselective organocatalytic process that uses the excited-state reactivity of chiral iminium ions to activate allenes by SET oxidation. The ensuing allene cation radicals participate in stereocontrolled cascade reactions to deliver chiral bicyclic scaffolds with good enantioselectivity and exquisite diastereoselectivity. **Density Functional Theory (DFT)** calculations support a mechanism that combines the peculiar chemistry of allene radical cations with polar reactivity.

Keywords: allene; cascade process; enantioselective organocatalysis; photochemistry; radical chemistry

There is increasing interest in allene chemistry.^[1] Once seen as exotic and hard to access,^[2] allenes are now recognised as suitable substrates for many synthetically useful transformations. They have been successfully used in cycloaddition reactions,^[3] radical processes,^[4] and metal-catalysed transformations.^[5] Allene chemistry has also been applied in natural products synthesis,^[1b,6] while enantioselective catalytic variants have been developed applying both metal-based strategies^[7] and organocatalysis.^[8]

The activation of allenes by single-electron transfer (SET) oxidation may offer new reactivity patterns to further expand the synthetic potential of these substrates. However, this activation strategy has been scarcely explored^[9] and has found limited synthetic utility to date. The few reported examples, which rely upon electrochemical methods^[10] or UV-based

photochemistry^[11] to trigger the SET oxidation of allenes, all suffer from regioselectivity issues and considerable limitations in scope. These restrictions mainly originate from the unique reactivity of the allene cation radicals $1^{+\bullet}$, which are generated upon SET oxidation of allenes **1** (**Scheme 1a**).



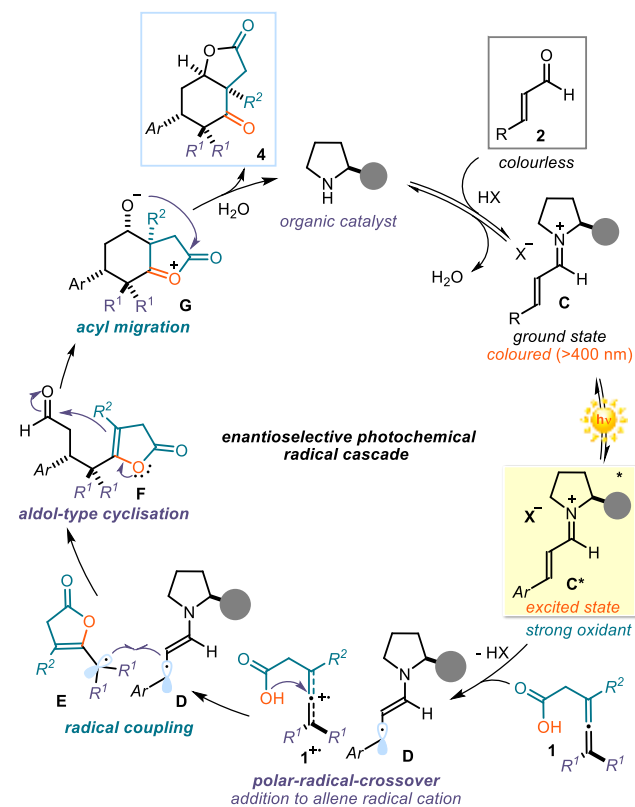
Scheme 1. a) Accessing allene cation radicals $1^{+\bullet}$ by single-electron transfer (SET) oxidation of allenes, and the competing reaction pathways available to these reactive intermediates. b) Proposed asymmetric radical cascade reaction based on the SET activation of allenic acids **1** by the excited iminium ions C^* .

These highly reactive intermediates $1^{+\bullet}$ are distonic radical cations, where the positive charge mainly resides on the central allene carbon, while the spin density is located on the other two carbon atoms.^[11c,d] A main reactivity path exploits the propensity of $1^{+\bullet}$ to undergo nucleophilic additions.^[11] As expected from the charge distribution, this process generally takes place at the central allene carbon, and delivers a more stable substituted allyl-type radical **A** (path *i* in **Scheme 1a**). The ensuing radical trap can then take place at both C-termini of **A**, potentially creating a problem of regioselectivity. A competing pathway available to the allene cation radical $1^{+\bullet}$ is the deprotonation at the terminal carbon, which leads to a reactive propargyl radical **B** (path *ii* in **Scheme 1a**). The multiple reactive manifolds available to $1^{+\bullet}$ highlight the difficulty of taming their reactivity, which is why complex mixtures of products are generally obtained.^[10,11]

Recently, our laboratories identified a new photochemical catalytic mode of substrate activation that exploits the excited-state reactivity of chiral iminium ions **C** to enable asymmetric transformations previously inaccessible via ground-state organocatalytic pathways.^[12] We found that iminium ions **C**, generated upon condensation of a chiral secondary amine catalyst and a α,β -unsaturated aldehyde **2**, are powerful oxidants in their electronically excited state, and they can activate suitable substrates by SET oxidation. This strategy allowed us to develop a variety of enantioselective transformations,^[12] including cascade reactions.^[13] We envisioned that the photochemistry of iminium ions could be used to activate allenes **1** and obtain reactive allene cation radicals $1^{+\bullet}$ upon SET oxidation (**Scheme 1b**). In addition, by using an allene substrate **1** adorned with a suitable oxygen-centred nucleophilic handle,^[14] we sought to address the reactivity challenges connected with the chemistry of $1^{+\bullet}$. This substrate **1** should selectively trigger an intramolecular nucleophilic addition into the central allene carbon, thus preventing undesired pathways. This step would produce a substituted double-bond moiety within intermediate **E** that would be capable of triggering a cascade process, leading to complex cyclic scaffolds.

Scheme 2 details our proposed strategy to develop an enantioselective radical cascade enabled by SET activation of allenes. We envisioned a catalytic cycle where the condensation of a chiral amine catalyst with enal **2** would form the coloured iminium ion intermediate **C**. Selective excitation with a single high-power (HP) light-emitting diode (LED) turns **C** into a strong oxidant **C*** (estimated reduction potential $E_{C^*/D} \approx +2.4$ V vs. Ag/Ag⁺ in CH₃CN).^[12a] The photo-excited iminium ion **C*** can oxidise the allene substrate **1** bearing a nucleophilic acid moiety. This is because these substrates have an oxidation potential ranging from +1.76 to +2.28V (vs. Ag/AgCl in CH₃CN, see section D in the Supporting Information for details). The SET activation of allene **1** would consequently form the chiral 5π -electron intermediate

D and the allene cation radical $1^{+\bullet}$. The acidic moiety within $1^{+\bullet}$, acting as a nucleophile, would then trigger a polar-radical-crossover addition onto the central carbon of the allene radical cation to afford the tertiary radical **E**. A stereo-controlled radical coupling with **D** would afford intermediate **F**. This species contains a reactive β,γ -unsaturated lactone moiety that, acting as an enolate equivalent, could trigger an aldol-type cyclisation to afford **G**. An acyl migration step would then afford the final product of the cascade, namely the complex bicyclic lactone **4**.



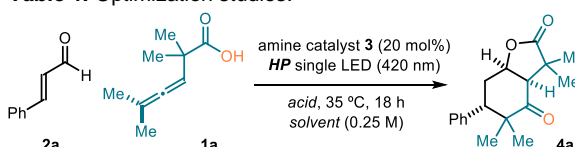
Scheme 2. Mechanistic proposal for the photo-organocatalytic enantioselective radical cascade triggered by the SET activation of allenic acids **1**.

The feasibility of the photochemical plan was evaluated by exploring the reaction of cinnamaldehyde **2a** catalysed by the *gem*-difluorinated diarylprolinol silylether **3**, which secured the formation of the chiral iminium ion (Table 1). The experiments were conducted in acetonitrile (CH₃CN), under irradiation by a single high-power (HP) LED ($\lambda_{\text{max}} = 420$ nm) with an irradiance of 90 mW/cm², as controlled by an external power supply (full details of the illumination set-up are reported in the Supporting Information, Figure S1). Allenic acid **1a**^[14] was selected as the model substrate because of its oxidation potential ($E_{p^{\bullet}/1a} = +2.28$ V vs Ag/AgCl in CH₃CN), which makes it prone to SET activation from the excited iminium ion. Gratifyingly, we observed that TFA (25 mol%), which served the dual role of facilitating iminium ion formation and triggering the aldol-type cyclisation of intermediate **F** into **G** (see **Scheme 2**), successfully enabled the overall cascade process (entry

1). The complex bicyclic product **4a** was formed with moderate chemical yield and enantioselectivity, but with full control over the relative stereochemistry.

We reasoned that Lewis acids could provide an additional means to assist iminium ion formation^[12d] while promoting the overall radical cascade. Accordingly, the use of zinc(II) triflate (25 mol%) provided product **4a** with improved efficiency (entry 2, 55% yield, 60% ee, full diastereocontrol). Triflates of trivalent metals, such as Sc(OTf)₃, were completely ineffective (entry 3). Increasing the amount of Zn(OTf)₂ (entry 4) or using reaction media other than CH₃CN did not improve the efficiency of the cascade process (entries 5 and 6). With the aim of further increasing the stereocontrol, we used the more encumbered amine catalyst **3b**, which however afforded largely inferior results (entry 7). Control experiments indicated that the Lewis acid co-catalyst, the organic catalyst, and visible light irradiation were all essential for the reaction to proceed (entries 8-10).

Table 1. Optimization studies.^[a]

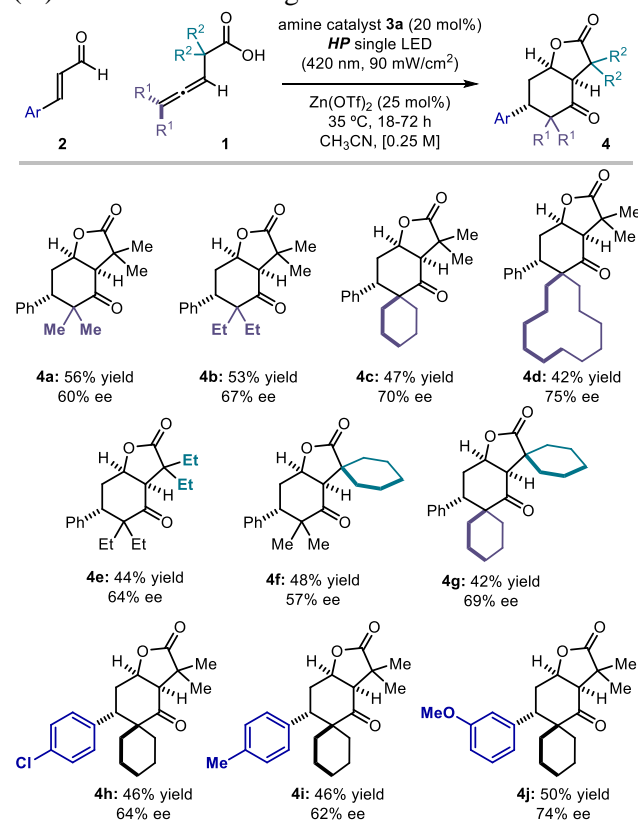


Entry	3	acid [mol%]	Solvent	4a yield [%] ^[b]	ee [%] ^[c]
1	a	TFA (25)	CH ₃ CN	44	54
2	a	Zn(OTf) ₂ (25)	CH ₃ CN	55	60
3	a	Sc(OTf) ₃ (25)	CH ₃ CN	0	-
4	a	Zn(OTf) ₂ (50)	CH ₃ CN	45	54
5	a	Zn(OTf) ₂ (50)	DCE	33	54
6	a	Zn(OTf) ₂ (50)	Benzene	32	48
7	b	Zn(OTf) ₂ (25)	CH ₃ CN	29	42
8 ^[d]	a	Zn(OTf) ₂ (25)	CH ₃ CN	0	-
9	a	none	CH ₃ CN	0	-
10	none	Zn(OTf) ₂ (25)	CH ₃ CN	0	-

^[a] Reactions performed on a 0.1 mmol scale at 35 °C for 18 h using 0.40 mL of solvent under illumination by a single high-power (HP) LED ($\lambda_{\text{max}} = 420 \text{ nm}$) with an irradiance of 90 mW/cm²; **4a** formed as a single diastereoisomer (d.r. > 19:1); the diastereoisomeric ratio (d.r.) was inferred by ¹H NMR analysis of the crude mixture. ^[b] Yields of isolated product **4a** after purification by flash column chromatography. ^[c] Enantiomeric excess determined by HPLC analysis on a chiral stationary phase. ^[d] No light. TFA: trifluoroacetic acid; TDS: thexyl-dimethylsilyl; DCE: 1,2-dichloroethane.

Adopting the optimised conditions described in Table 1, entry 2, we evaluated the generality of the photochemical radical cascade process (Scheme 3). As for the scope of the allenic acid substrates **1**, we

observed an improved enantioselectivity when bulkier substituents were installed onto the allene moiety (adducts **4a-d**). Changing the steric profile of the substituents at the alpha position to the acid moiety within **1** did not significantly affect the reactivity and stereoselectivity of the cascade (products **4e-f**). The tetracyclic adduct **4g**, bearing two spiro quaternary carbons, could also be successfully synthesised. As for the scope of the enal substrate **2**, moderately electron-withdrawing (**4h, 4j**) and electron-donating groups (**4i**) on the aromatic ring were tolerated well.

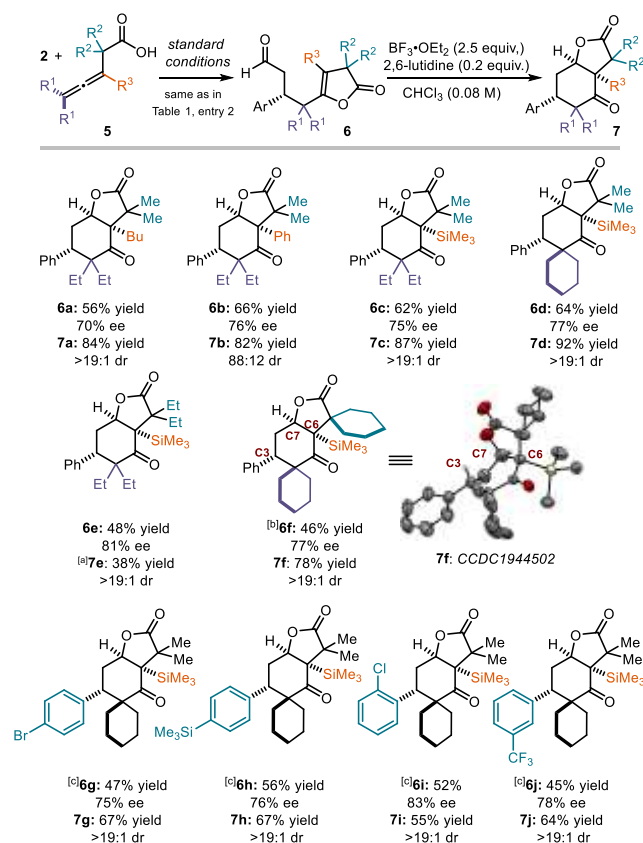


Scheme 3. Survey of the allenic acids **1** and enals **2** that can participate in the photochemical asymmetric cascade process. Reactions performed on 0.1 mmol scale using 3 equiv. of **2**. Yields and enantiomeric excesses of the isolated products **4** are indicated below each entry (average of two runs per substrate). All products were formed as single diastereoisomers (d.r. > 19:1); the diastereoisomeric ratio (d.r.) was inferred by ¹H NMR analysis of the crude mixture.

As a limitation of the system, and in consonance with our previous studies,^[12,13] aliphatic enals were not suitable substrates as the reactivity was completely inhibited. Remarkably, products **4** were all obtained as single diastereoisomers, since no minor isomers could be detected by ¹H NMR analysis of the crude reaction mixtures.

We then explored the tendency of substrates with a tetrasubstituted allene moiety (**5**) to participate in the cascade process (Scheme 4). While the light-mediated radical manifold was operative, the presence of a fourth substituent on the allene moiety greatly lowered the nucleophilicity of intermediate **6** (which corresponds to **F** in the overall mechanistic picture in

Scheme 2). Indeed, **6** could not cyclise further, thus interrupting the cascade. Nevertheless, treatment of the isolable intermediates **6** with $\text{BF}_3 \cdot \text{OEt}_2$ (2.5 equiv.) in the presence of 2,6-lutidine (20 mol%)^[15] smoothly delivered the complex products **7** containing a quaternary stereocenter α to the carbonyl function.



Scheme 4. Survey of tetrasubstituted allenic acids **5** that can participate in the cascade process with enals **2**. Standard conditions are those reported in Table 1, entry 2. Reactions performed on 0.1 mmol scale using 3 equiv. of **2**. The second cyclisation step was performed on the isolated pure adducts **6**. Yields and enantiomeric excesses of the isolated products **6** and **7** are indicated below each entry (average of two runs per substrate). Diastereomeric ratio (dr) was inferred from ^1H NMR analysis of the crude mixture. ^[a] Reaction performed using 5 equiv. of $\text{BF}_3 \cdot \text{OEt}_2$. ^[b] Reaction performed using PrCN instead of CH_3CN as the solvent. ^[c] Reaction performed with TFA (60 mol%) instead of $\text{Zn}(\text{OTf})_2$ and using CH_3CN [0.5 M] as the solvent.

We then studied the synthetic applicability of this two-step procedure (Scheme 4). The effect of the substituents on allenic acids **5** mirrors the trends observed for substrates **1**, since larger groups modestly improved yields and enantioselectivities. Alkyl (product **7a**), aryl (**7b**), and trimethylsilyl (**7c**) groups are tolerated at the R^3 position within substrates **5**. Concerning the enal substrates **2**, strongly electron-withdrawing groups are tolerated on the aromatic ring (**7j**). Notably, synthetically useful groups, which can undergo further functionalisation, were also tolerated. These included halogens (**7g**, **7i**) and trimethylsilyl (**7h**). The diastereoselectivity of the ring closure was

generally excellent (>19:1 dr), with the exception of product **7b** (88:12 dr).

Crystals of compound **7f** were suitable for X-ray crystallographic analysis,^[16] which secured the absolute and relative configuration of the products.

The second part of the cascade process involves the aldol cyclisation leading to products **4** from intermediates of type **F** (see Scheme 2) and products **7** from intermediates **6**. It is mechanistically interesting, especially when considering the full diastereoselectivity observed. The intermolecular aldol reaction of enol esters with aldehydes promoted by Lewis acids has been described by Mukayama.^[17] However, its diastereoselectivity in the intramolecular variant has never been examined. We thus resorted to Density Functional Theory (DFT) calculations to gain more insight on the origin of the relative stereocontrol (Figure 1).^[18]

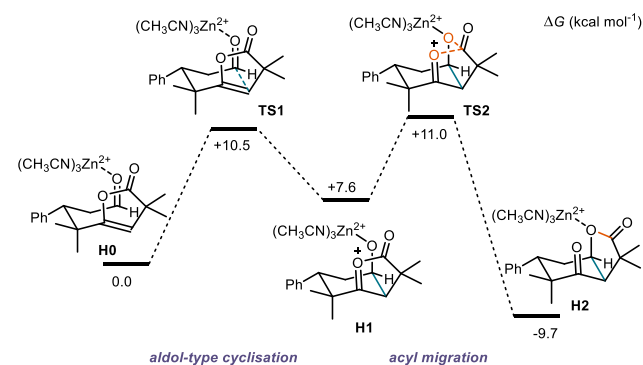


Figure 1. Computed free-energy profile of the aldol-type cyclisation of the aldehyde intermediate **F** deriving from the photochemical coupling of the allene carboxylic acid **1a** and cinnamaldehyde **2a**. Relative Gibbs free energies at 298 K are reported in kcal mol^{-1} .

$\text{Zn}(\text{NCCH}_3)_3^{2+}$, acting as a Lewis acid,^[19] coordinates the aldehyde oxygen, thereby enhancing the electrophilicity of the carbonyl carbon. In the reactive conformation of this Lewis acid-substrate adduct (**H0**), the forming cyclohexane ring is in a chair-like conformation where the aldehyde oxygen and the oxygen of the enol ether are in pseudo-axial positions while the phenyl ring occupies an equatorial site. The aldol-type addition is predicted to be a stepwise process: first, an acyloxonium intermediate **H1** is formed through transition state **TS1** ($\Delta G^\ddagger = 10.5 \text{ kcal mol}^{-1}$). This reaction is endergonic ($\Delta G = +7.6 \text{ kcal mol}^{-1}$), but the acyl transfer via **TS2** is exergonic and it provides the thermodynamic driving force for the overall process (total $\Delta G = -9.7 \text{ kcal mol}^{-1}$ from **H0** to **H2**). For the crucial acyl transfer process to take place, both oxygen atoms (origin and terminus of the migration) must be in close proximity, which is only possible if they are in an 1,3-diaxial-like relationship. This stereochemical requirement determines the experimentally observed diastereoselectivity for the *cis*-fused bicyclic system.^[20]

In summary, we exploited the photochemical activity of chiral iminium ions to activate allenes by SET oxidation. The propensity of allene radical cations to undergo addition of nucleophiles was crucial to design a cascade process leading to complex, polysubstituted bicyclic lactones. We expect that this activation strategy may offer fresh opportunities to further expand the synthetic potential of allenes.

Experimental Section

General Procedure for the Photochemical Enantioselective Cascade of Allenic Acids 1.

A Schlenk flask (approximate diameter: 15 mm) was charged with the appropriate allenic acid **1** (0.1 mmol), the chiral amine catalyst **3a** (14.1 mg, 0.02 mmol, 0.20 equiv.), the enal **2** (0.30 mmol, 3.0 equiv.), Zn(OTf)₂ (9.1 mg, 0.025 mmol, 0.25 equiv.), and CH₃CN (400 μL). The mixture was degassed by three cycles of freeze-pump-thaw and kept under an atmosphere of argon. The Schlenk flask was placed into an aluminium block on a 3D-printed holder, fitted with a 420 nm high-power single LED. The irradiance was fixed at 90±2 mW/cm², as controlled by an external power supply and measured using a photodiode light detector at the start of each reaction. The reaction was stirred for 16-24 h and then flushed through a plug of silica gel using Et₂O as the eluent. Volatiles were removed under reduced pressure and the resulting solids were directly loaded on a flash chromatography column (silica gel) and eluted to obtain the purified products **4**.

(3aR,6S,7aR)-3,3,5,5-Tetramethyl-6-phenylhexahydrobenzofuran-2,4-dione (4a)

The reaction of 2,2,5-trimethylhexa-3,4-dienoic acid (**1a**) with cinnamaldehyde (**2a**) was performed according to the general procedure (reaction time: 18 hours). The title product was obtained upon flash chromatography purification (eluent: hexanes:EtOAc 90:10) in the form of an off-white solid (16.0 mg, 56%, average of two runs, 60% ee).

The enantiomeric excess was determined by UPC² analysis on a chiral stationary phase (Daicel Chiralpak IC-3, gradient: CO₂:MeOH from 100:0 to 60:40 over 4.0 minutes, flow rate: 3.0 mL/min, λ = 207 nm, τ_{major} = 2.45 min, τ_{minor} = 2.55 min). [α]_D²⁶ = +4.2 (c = 0.13, CHCl₃, 60% ee). ¹H NMR (300 MHz, CDCl₃): δ 7.36 – 7.26 (m, 3H), 7.17 – 7.10 (m, 2H), 5.13 (dt, J = 7.2, 3.3 Hz, 1H), 3.14 (dd, J = 12.6, 3.3 Hz, 1H), 2.97 (d, J = 7.2 Hz, 1H), 2.47 (ddd, J = 15.0, 12.6, 3.3 Hz, 1H), 2.35 (dt, J = 15.0, 3.3 Hz, 1H), 1.45 (s, 3H), 1.30 (s, 3H), 1.02 (s, 3H), 0.95 (s, 3H). ¹³C NMR (126 MHz, CDCl₃): δ 213.4, 180.9, 139.4, 129.4, 128.2, 127.2, 74.7, 55.4, 48.6, 45.0, 43.5, 29.9, 28.2, 24.7, 23.0, 21.3. HRMS (ESI) m/z Calculated for C₁₈H₂₂NaO₃⁺ [M+Na]⁺: 309.1461, found 309.1468.

Acknowledgements

Financial support was provided by MICIU (CTQ2016-75520-P), the AGAUR (Grant 2017 SGR 981), and the European Research Council (ERC-2015-CoG 681840 - CATA-LUX).

References

- [1] a) N. Krause, A. S. K Hashmi, *Modern Allene Chemistry*, Wiley-VCH, Weinheim, **2009**; b) S. Ma, *Chem. Rev.* **2005**, *105*, 2829–2871; c) E. Soriano, I. Fernandez, *Chem. Soc. Rev.* **2015**, *43*, 3041–3105.
- [2] For overviews on the synthesis of allenes, see: a) S. Ma, S. Yu, *Chem. Comm.* **2011**, *47*, 5384–5418; b) L. Brandsma, *Synthesis of Acetylenes, Allenes and Cumulenes*, Elsevier, Oxford, **2004**.
- [3] For a review on [4+2] and [4+3] cycloadditions, see: a) F. Lopez, J. L. Mascareñas, *Chem. Soc. Rev.* **2014**, *43*, 2904–2915. For a review on [2+2] cycloadditions: b) B. Alcaide, P. Almendros, C. Aragoncillo, *Chem. Soc. Rev.* **2010**, *39*, 783–816. For a review on [2+2+1] cyclizations of allenes, see: c) S. Kitagaki, F. Inagaki, C. Mukai, *Chem. Soc. Rev.* **2014**, *43*, 2956–2978.
- [4] a) G. Qiu, J. Zhang, K. Zhou, J. Wu, *Tetrahedron* **2018**, *74*, 7290–7301. For recent examples, see: b) N. Lu, Z. Zhang, N. Ma, C. Wu, G. Zhang, Q. Liu, T. Liu, *Org. Lett.* **2018**, *20*, 4318–4322; c) S. Araia, K. Matsumoto, A. Nishida, *Tetrahedron* **2019**, *75*, 1145–1148.
- [5] a) S. Ma, *Acc. Chem. Res.* **2003**, *36*, 701–712; b) A. L. Reznichenko, K. C. Hultsch, V. P. Ananikov, M. Tanaka, *Top. Organomet. Chem.*, **2011**, *43*, 51–114; c) R. A. Widenhoefer *Transition Metal-Catalyzed Hydroarylation of Allenes in Catalytic Hydroarylation of Carbon-Carbon Multiple Bonds*, Wiley-VCH, Weinheim, **2018**.
- [6] For a review: a) S. Ma, S. Yu, *Angew. Chem. Int. Ed.* **2012**, *51*, 3074–3112. For selected examples: b) J. E. Sears, T. J. Barker, D. L. Boger, *Org. Lett.* **2015**, *17*, 5460–5463; c) J. A. Marshall, M. P. Bourbeau, *J. Org. Chem.* **2002**, *67*, 2751–2754; d) K. K. D. Amarasinghe, J. Montgomery, *J. Am. Chem. Soc.* **2002**, *124*, 9366–9367; e) P. A. Wender, L. Zhang, *Org. Lett.* **2000**, *2*, 2323–2326; f) J. D. Ha, J. K. Cha, *J. Am. Chem. Soc.* **1999**, *121*, 10012–10020.
- [7] For reviews, see: a) M. Holmes, L. A. Schwartz, M. J. Krische, *Chem. Rev.* **2018**, *118*, 6026–6052; b) P. Koschker, B. Breit, *Acc. Chem. Res.* **2016**, *49*, 1524–1536. For selected examples: c) Z. Chen, V. M. Dong, *Nature Commun.* **2017**, *8*, 784; d) T. Ohmura, H. Taniguchi, M. Sugimoto, *J. Am. Chem. Soc.* **2006**, *128*, 13682–13683.
- [8] For selected recent examples: a) P. Elsner, L. Bernardi, G. Dela Salla, J. Overgaard, K. A. Jørgensen, *J. Am. Chem. Soc.* **2008**, *130*, 4897–4905; b) I. P. Andrews, O. Kwon, *Chem. Sci.* **2012**, *3*, 2510–2514; c) A. Hölzl-Hobmeier, A. Bauer, A. Vieira Silva, S. M. Huber, C. Bannwarth, T. Bach,

- Nature* **2018**, *564*, 240–243; d) J.-S. Lin, T.-T. Li, G.-Y. Jiao, Q.-S. Gu, J.-T. Cheng, L. Lv, X.-Y. Liu, *Angew. Chem. Int. Ed.* **2019**, *58*, 7092–7096; *Angew. Chem.* **2019**, *131*, 7166–7170.
- [9] Photo-induced SET oxidation strategies have been extensively used in synthetic photochemistry to activate simple alkenes, but the activation of allenes has remained largely understudied. For a review on SET oxidation of alkenes, see: a) K. A. Margrey, D. A. Nicewicz, *Acc. Chem. Res.* **2016**, *49*, 1997–2006; for selected examples: b) J.-M. M. Grandjean, D. A. Nicewicz, *Angew. Chem. Int. Ed.* **2013**, *52*, 3967–3971; *Angew. Chem.* **2013**, *125*, 4059–4063; c) M. A. Zeller, M. Riener, D. A. Nicewicz, *Org. Lett.* **2014**, *16*, 4810–4813; d) N. A. Romero, D. A. Nicewicz, *J. Am. Chem. Soc.* **2014**, *136*, 17024–17035.
- [10] a) J. Y. Becker, B. Zinger, *Tetrahedron* **1982**, *38*, 1677–1682; b) J. Y. Becker, B. Zinger, *J. Chem. Soc. Perkin Trans. 2*, **1982**, 395–401; c) G. Schlegel, H. J. Schäfer, *Chem. Ber.* **1983**, *116*, 960–969.
- [11] a) M. W. Klett, R. P. Johnson, *Tetrahedron Lett.* **1983**, *24*, 1107–1110; b) M. W. Klett, R. P. Johnson, *J. Am. Chem. Soc.* **1985**, *107*, 6615–6620; c) K. Somekawa, K. Haddaway, P. S. Mariano *J. Am. Chem. Soc.* **1984**, *106*, 3060–3062; d) K. Haddaway, K. Somekawa, P. Fleming, J. A. Tossell, P. S. Mariano, *J. Org. Chem.*, **1987**, *52*, 4239–4253; e) D. R. Arnold, K. A. McManus, M. S. W. Chan, *Can. J. Chem.* **1997**, *75*, 1055–1075; f) D. Mangion, D. R. J. Arnold, T. S. Cameron, K. N. Robertson, *Chem. Soc. Perkin Trans. 2*, **2001**, 48–60
- [12] a) M. Silvi, C. Verrier, Y. P. Rey, L. Buzzetti, P. Melchiorre, *Nat. Chem.* **2017**, *9*, 868–873; b) C. Verrier, N. Alandini, C. Pezzetta, M. Moliterno, L. Buzzetti, H. B. Hepburn, A. Vega-Peñaloza, M. Silvi, P. Melchiorre, *ACS Catal.* **2018**, *8*, 1062–1066; c) D. Mazzarella, G. E. M. Crisenza, P. Melchiorre, *J. Am. Chem. Soc.* **2018**, *140*, 8439–8443. For a review, see: d) M. Silvi, P. Melchiorre, *Nature* **2018**, *554*, 41–49.
- [13] a) Ł. Woźniak, G. Magagnano, P. Melchiorre, *Angew. Chem. Int. Ed.* **2018**, *57*, 1068–1072; *Angew. Chem.* **2018**, *130*, 1080–1084; b) P. Bonilla, Y. P. Rey, C. M. Holden, P. Melchiorre, *Angew. Chem. Int. Ed.* **2018**, *57*, 12819–12823; *Angew. Chem.* **2018**, *130*, 13001–13005.
- [14] As discussed in the Supporting Information, the β -allenyl carboxylic acid substrates **1** are prepared in one operation by the Ireland-Claisen rearrangement of propargyl esters: a) J. E. Baldwin, P. A. R. Bennett, A. K. Forrest, *J. Chem. Soc., Chem. Commun.* **1987**, 250–251. The [3,3] rearrangement of propargyl derivatives leading to allenes is known as the Saucy-Marbet reaction, see: b) D. Tejedor, G. Méndez-Abt, L. Cotos, F. García-Tellado, *Chem. Soc. Rev.* **2013**, *42*, 458–471.
- [15] The role of 2,6-lutidine is presumably to neutralise small amounts of HBF₄ generated upon hydrolysis of BF₃•OEt₂ by adventitious moisture.
- [16] Crystallographic data for compound **7f** has been deposited with the Cambridge Crystallographic Data Centre, accession number CCDC 1944502.
- [17] a) T. Mukaiyama, T. Izawa, K. Saigo, *Chem. Lett.* **1974**, 323–326; b) M. Yanagisawa, T. Shimamura, D. Iida, J. Matsuo, T. Mukaiyama, *Chem. Pharm. Bull.* **2000**, *48*, 1838–1840. See also: b) Y. Masuyama, T. Sakai, T. Kurusu, *Tetrahedron Lett.* **1993**, *34*, 653–656; c) A. Yanagisawa, N. Kushiara, K. Yoshida, *Org. Lett.* **2011**, *13*, 1576–1578
- [18] Level of theory for geometry optimisation and frequency calculations: B3LYP/6-31+G(d) (for C, H, N, O), LANL2TZ/LANL2 (for Zn), IEF-PCM (CH₃CN); for single-point electronic energies: B3LYP-D3BJ/6-311+G(2d,2p) (for C, H, N, O), LANL08+/LANL2 (for Zn), IEF-PCM (CH₃CN). See the Supporting Information for full computational details.
- [19] Zn(OTf)₂ is almost completely dissociated in CH₃CN solutions, as evinced by an association constant as low as $K_a = 3 \cdot 10^{-2} \text{ M}^{-1}$, which was measured by electroanalytical studies, see: T. Fujinaga, I. Sakamoto, *J. Electroanal. Chem.* **1976**, *73*, 235–246. Therefore, solvent-coordinated Zn²⁺ was considered as the Lewis acid in the theoretical calculations. As for the solvent, an electrostatic model (IEF-PCM) has been employed to reproduce bulk solvation effects.
- [20] For additional mechanistic discussion and analysis of alternative pathways, see the Supporting Information, section F.

Photo-Organocatalytic Enantioselective Radical Cascade Enabled by Single-Electron Transfer Activation of Allenes

Adv. Synth. Catal. **Year**, *Volume*, Page – Page

Luca Alessandro Perego, Pablo Bonilla, and Paolo Melchiorre*

